



HAL
open science

Heats of Adsorption of CO on a Cu/Al₂O₃Catalyst Using FTIR Spectroscopy at High Temperatures and under Adsorption Equilibrium Conditions

Olivier Dulaurent, Xavier Courtois, Vincent Perrichon, Daniel Bianchi

► **To cite this version:**

Olivier Dulaurent, Xavier Courtois, Vincent Perrichon, Daniel Bianchi. Heats of Adsorption of CO on a Cu/Al₂O₃Catalyst Using FTIR Spectroscopy at High Temperatures and under Adsorption Equilibrium Conditions. *Journal of Physical Chemistry B*, 2000, 104 (25), pp.6001 - 6011. 10.1021/jp9943629 . hal-03106888

HAL Id: hal-03106888

<https://hal.science/hal-03106888>

Submitted on 12 Jan 2021

HAL is a multi-disciplinary open access archive for the deposit and dissemination of scientific research documents, whether they are published or not. The documents may come from teaching and research institutions in France or abroad, or from public or private research centers.

L'archive ouverte pluridisciplinaire **HAL**, est destinée au dépôt et à la diffusion de documents scientifiques de niveau recherche, publiés ou non, émanant des établissements d'enseignement et de recherche français ou étrangers, des laboratoires publics ou privés.

Heats of Adsorption of CO on a Cu/Al₂O₃ Catalyst Using FTIR Spectroscopy at High Temperatures and under Adsorption Equilibrium Conditions

Olivier Dulaurent, Xavier Courtois, Vincent Perrichon, and Daniel Bianchi*

Laboratoire d'Application de la Chimie à l'Environnement (LACE), UMR 5634, Université Claude Bernard, Lyon-I, Bat. 308, 43 Bd du 11 Novembre 1918, 69622 Villeurbanne, France

Abstract:

The adsorption of CO on a 4.7% Cu/Al₂O₃ catalyst either reduced or oxidized is studied using the FTIR spectra recorded at adsorption temperatures T_a in the range 298-740 K and with two constant partial pressures P_a (10^3 and 10^4 Pa). On the reduced solid and at $T_a = 300$ K a single IR band is detected at 2092 cm^{-1} ascribed to a linear CO species (denoted by L_0) on Cu° particles. The FTIR spectra lead to the determination of the evolution of the coverage θ of the L_0 species with T_a for the two CO pressures. In the temperature range $380\text{ K} > T_a > 480\text{ K}$, the curves $\theta = f(T_a)$ for the two CO pressures are in very good agreement with Temkin's adsorption model. Moreover, it is shown that, in the range 300-600 K, the curves are in agreement with an adsorption model considering (a) an immobile adsorbed species and (b) a linear decrease in the heat of adsorption with the coverage θ in the range 0-1. This leads to the determination of the heat of adsorption E_θ , at various coverages θ from $E_0 = 82\text{ kJ/mol}$ at $\theta = 0$ to $E_1 = 57\text{ kJ/mol}$ at $\theta = 1$. It is shown that these values are similar to those obtained using the Clausius-Clapeyron equation. On the oxidized Cu/Al₂O₃ catalyst, an IR band is detected at 2120 cm^{-1} at 300 K. Its intensity increases either with time on stream in 1% CO/He or with increase in T_a . This IR band is ascribed to a linear CO species (denoted by L_1) on Cu^+ sites and the increase in its intensity is assigned to the reduction of the copper oxide surface. The maximum in the superficial concentration of the Cu^+ sites is obtained after reduction in 1% CO/He at 473 K. This allows the determination of the heats of adsorption of L_1 species at various coverages which linearly vary with θ from $E'_0 = 115\text{ kJ/mol}$ at $\theta = 0$ to $E'_1 = 58\text{ kJ/mol}$ at $\theta = 1$. The two L species are present simultaneously on the surface for an incomplete reduction of the solid, and it is shown that this does not significantly affect the heats of adsorption of the two adsorbed species. Moreover, the aging of the reduced catalyst has no effect on the heats of adsorption of the L_0 and L_1 species but leads to the detection of a new IR band at 2003 cm^{-1} ascribed to a bridged CO species on Cu° sites. The heat of adsorption of this species is strongly higher than those of the two L species varying with the coverage from 130 kJ/mol at $\theta = 0$ to 78 kJ/mol at $\theta = 1$. Finally, it is shown that the heats of adsorption of the L_0 and L_1 species are in accord with the literature data on the stability of the two adsorbed species in the course of a desorption at room temperature.

1. Introduction

The heats of adsorption (abbreviation: H.A. or Hs.A.) of the adsorbed species formed by the adsorption of CO on supported metal catalysts and their evolutions with coverage θ (denoted E_θ with $0 \leq \theta \leq 1$) are an important characteristic of these catalytic systems because the E_θ

values quantify the coverage of the sites under adsorption equilibrium conditions. However, the Hs.A. are less studied than other parameters such as the amounts and the nature of the adsorbed species formed, due to experimental difficulties. For instance, temperature programmed desorption methods (TPD) which enable the determination of the desorption activation energies (equal to E_{θ} for the CO/metal system) on single crystals are not well adapted for supported metal catalysts because it is difficult to achieve TPD experimental conditions free of the influence of diffusion and readsorption.¹ This explains the interest in microcalorimetric methods^{2,3} which provide either the integral or the differential Hs.A. However, in the case of the formation of several adsorbed CO species this method provides an average of the Hs.A. E_{θ} can also be determined using the Clausius-Clapeyron equation from the amount of adsorbed CO species measured at various adsorption pressures P_a and temperatures T_a .^{4,5} The accuracy of the experimental methods providing the adsorbed quantities must be very high; otherwise the values of E_{θ} are strongly affected. Moreover, if several adsorbed CO species are formed, the analytical methods must be able to differentiate the amount of each adsorbed species; otherwise, at best, an average of the Hs.A. can be obtained. This is the case for single crystals and supported model particles using IRAS spectroscopy^{6,7} as the analytical method. We have shown previously that similar experiments can be performed with supported metal catalyst using an adapted IR cell⁸ that is an alternative analytical solution to the DRIFT cells.⁹ This cell allows the studies of CO species adsorbed on supported metal catalysts at adsorption equilibrium conditions and in wide pressure and temperature ranges. In the case of Pt-containing catalysts and for a linear CO species,⁸ it has been shown that the FTIR spectra led to the determination of the evolution of θ as a function of T_a at a given adsorption pressure P_a (isobar). The curve $\theta = f(T_a)$ provided the Hs.A., E_{θ} , of the linear CO species at various coverages using an adsorption model.⁸ It has been shown¹⁰ that these E_{θ} values were in good accord with the isosteric Hs.A. using several isobars. The method using a single isobar has been also applied for the determination of the Hs.A. of a linear and of a bridged CO species formed on a Pd/Al₂O₃ catalyst¹¹ as a function of their respective coverages. In the present study the procedure is applied for the determination of the Hs.A. of CO on the reduced and then on the oxidized form of a Cu/Al₂O₃ catalyst.

There are several interests in the choice of this metal. The first is linked to the fact that the Hs.A. of CO on Cu single crystals and reduced supported copper catalysts are in the range 60-80 kJ/mol at low coverages¹² and decrease with increasing coverage.¹³ This means that the reduced Cu/Al₂O₃ solid may allow us to verify that the method of determination of the Hs.A. (experimental coverage and adsorption model) can be applied in the coverage range 0-1. On the supported metal catalysts previously studied^{8,10,11} the Hs.A. of the different adsorbed CO species at low coverages were mainly higher than 140 kJ/mol leading to a coverage in the range 0.3-0.5 even for high T_a values (700-800 K) and low P_a values (10³ Pa). There is a second interest in the choice of copper: the active sites of copper catalysts in several catalytic processes are the subject of controversial discussions and various questions^{12,14} are under investigation. One of these problems is the characterization of Cu⁰ and Cu⁺ sites using the CO adsorption. At 300 K, the adsorption of CO on these two sites leads to close IR bands due to linear CO species situated in the ranges 2130-2050 cm⁻¹ for Cu⁰ and 2140-2110 cm⁻¹ for Cu⁺.^{12,14,15} The assignment of an IR band to Cu⁰ or Cu⁺ sites is usually ascertained by its stability in the course of a desorption at room temperature. The CO species formed on Cu⁰ sites is considered less stable (the IR band disappears) than that formed on Cu⁺ sites (the IR band is slightly or moderately decreased).^{12,15-17} However, this difference in stability of the two CO species, which is only evaluated by the comparison of the intensities of the remaining IR bands after a given time of desorption, can be quantified measuring the Hs.A. of the two linear CO species at various coverages.

In the present study, we determine the Hs.A. of the two linear CO species formed on Cu⁰ (totally reduced Cu/Al₂O₃ solid), on Cu⁺ (oxidized and slightly reduced Cu/Al₂O₃ solid), and then in the presence of the two species (incomplete reduction of the oxidized Cu/Al₂O₃ solid). The effects of the sintering of copper particles on the Hs.A. of the adsorbed CO species on the Cu⁰ and Cu⁺ sites are presented. Moreover, the aging of the solid leads to the detection of a bridged CO species on Cu⁰ sites. The Hs.A. of this species at various coverages are also determined.

2. Experimental Section

A 4.7% Cu/Al₂O₃ (in wt %) catalyst was prepared using impregnation of alumina (Rhône-Poulenc 531P, BET of 115 m²/g) with an appropriate amount of an aqueous solution of Cu(NO₃)₂·3H₂O (Strem Chemicals). The solvent was evaporated slowly at 353 K, and after drying 12 h at 383 K, the solid was treated 6 h at 673 K in O₂ (100 cm³/min, heating rate 1 K/min). After cooling to room temperature in O₂ followed by a purge in N₂, the XRD analysis indicated that copper was present as CuO oxide. The solid was reduced in H₂, 6 h at 773 K (100 cm³/min, heating rate 1 K/min), cooled to 300 K in H₂, purged in N₂, and maintained in air before use. After these treatments the BET area was 104 m²/g. The copper loading was determined by inductively coupled plasma after dissolution of the catalyst. The temperature programmed reduction of the calcined solid after a treatment in O₂ at 673 K followed by a 1.5 h purge in Ar at 773 K (solid cooled in Ar to room temperature) was performed (20 K/min) using a 1% H₂/Ar mixture with a catharometer as detector. The dispersion of the reduced copper catalyst was determined via dissociative N₂O adsorption¹² (N₂O_(g) + 2Cu_s → N_{2(g)} + (Cu₂O)_s) at 363 K measuring the amounts of N₂O consumption and N₂ production in the course of the adsorption using an analytical system for transient experiments with a mass spectrometer as detector.⁸

For the FTIR study, the catalyst was compressed to form a disk ($\Phi = 1.8$ cm, $m = 40$ -90 mg) which was placed in the sample holder of a small internal volume stainless steel IR cell described elsewhere⁸ allowing in situ treatments (293-900 K) of the solid, at atmospheric pressure, with a gas flow rate in the range of 150-2000 cm³/min. Before the adsorption of CO, the solid was treated in situ (200 cm³/min) according to the following procedure: He, 298 K → He, 383 K → H₂, 383 K (1 h) → H₂, 523 K, (1 h) → H₂, 713 K (2 h) → He, 713 K (5 min) → He, 300 K. The same pellet of solid was used for several adsorption experiments, and before each adsorption the following pretreatments were performed: (a) for the oxidized solid, He, 713 K → O₂, 713 K (0.5 h) → He, 713 K, (0.5 h) → He, 300 K → CO adsorption (in some experiments the solid was cooled to 300 K in O₂ followed by 10 min in He before the CO adsorption); (b) for the reduced solid, He, 713 K → O₂, 713 K (0.5 h) → He, 713 K (0.5 h) → H₂, 713 K (0.5 h) → He, 713 K (0.5 h) → He, 300 K → CO adsorption. The CO adsorptions at various T_a were performed according to the following procedure: pretreated solid → He, 300 K → $x\%$ CO/He (total pressure = 1 atm, flow rate = 200 cm³/min, $x = 1$ or 10) → increase in T_a (5-10 K/min) up to $T_a < 713$ K while the FTIR spectra of the adsorbed species were recorded periodically. After the highest adsorption temperature, the solid was cooled in the presence of $x\%$ CO/He and the spectra were compared to those recorded in the course of the heating stage to reveal a possible modification of the catalyst during the CO adsorption at high temperatures.

3. Results

3.1. Temperature Programmed Reduction and Dispersion. The TPR profile (not shown) indicated two strong peaks of hydrogen consumption at $T_m = 550$ K and $T_m = 660$ K with a

third smaller peak at $T_m = 773$ K. The total amount of hydrogen consumption (in the temperature range 300-878 K) was $693 \mu\text{molH}_2/\text{g}$, which indicated that $\approx 94\%$ of the copper oxide assumed as CuO was reduced to Cu^\ominus . The approximate deconvolution of the three peaks led to the following percentages of H_2 consumed in each peak: 54%, 28% and 18%. Note that if the TPR experiment was performed in the range 300-1273 K the percentage of reduction was 104% ($770 \mu\text{mol}$ of H_2/g). However, in these conditions a fraction of the hydrogen consumption was due to the contribution of the alumina support as revealed by a blank experiment performed with the support alone (initially treated as the 4.7% $\text{Cu}/\text{Al}_2\text{O}_3$ catalyst) which indicated a small broad TPR peak with a maximum at 1023 K ($\approx 30 \mu\text{mol}$ of H_2/g of alumina). The TPR performed on the reduced solid (reoxidized during an initial treatment in O_2 at 673 K) did not indicate a strong modification of the TPR profile. Mainly the temperatures at the maximum of the peaks were modified (580, 640, and 740 K for the first, second, and third peaks, respectively). The above results lead to the conclusion that the copper oxide particles must be totally reduced during the FTIR analysis (H_2 , 1 atm, 713 K), and that there is no significant reduction of the bulk copper oxide before 473 K (see below).

The dissociative adsorption of N_2O at 363 K on the reduced catalyst using a 0.8% $\text{N}_2\text{O}/2\%$ Ar/He mixture indicated from the amount of N_2 formed a dispersion of 0.11 for the fresh reduced catalyst assuming a ratio $\text{Cu}/\text{N}_2 = 2$.¹² This value is lower than that determined by Dandekar and Vannice¹² (range ≈ 0.2 -0.5) on 5.1% Cu/SiO_2 and 4.9% $\text{Cu}/\text{Al}_2\text{O}_3$, but the solids were pretreated and reduced at lower temperatures (473 and 573 K) compared to the present study (713 K).

3.2. Adsorption of CO on the Reduced $\text{Cu}/\text{Al}_2\text{O}_3$ Solid. Figure 1 shows, for the 1% CO/He mixture, the FTIR spectra recorded on the reduced 4.7% $\text{Cu}/\text{Al}_2\text{O}_3$ catalyst in the course of the adsorption in the T_a range 300-600 K. At 300 K (spectrum a) a strong IR band is observed at 2092 cm^{-1} alongside a weak shoulder in the range 2080 - 2060 cm^{-1} . These IR bands are ascribed to linear CO species on Cu^\ominus particles (denoted by L_0). It seems that there is an agreement in the literature to consider according to the various studies of Pritchard et al.²⁰ (see references therein) and to the IR spectra of Cu_nCO complexes (n ranging from 1 to 4),²¹ that on reduced copper catalysts^{15,18,19} (a) an IR band below 2100 cm^{-1} indicates that the L_0 species is formed on densely packed surface $\text{Cu}(111)$, $\text{Cu}(100)$, and $\text{Cu}(110)$ (for instance on $\text{Cu}(100)$ an IR band at 2086 cm^{-1} is observed at high coverage by IRAS²²), (b) an IR band in the range 2110 - 2100 cm^{-1} indicates that the L_0 species is formed on stepped surfaces, and (c) an IR band at higher wavenumbers is assigned to L_0 species formed on defect-rich surfaces¹⁸ or isolated Cu^\ominus .¹⁵ The position of the main IR band at 2092 cm^{-1} in Figure 1 is similar to that (2099 cm^{-1}) observed on a reduced (573 K) 4.9% $\text{Cu}/\text{Al}_2\text{O}_3$ catalyst¹² which was assigned to Cu^\ominus sites. Considering the above remark on the assignment of the IR band on reduced copper containing solids, we assign the shoulder at 2080 - 2060 cm^{-1} to reduced copper particles with a specific orientation. Some authors, however, consider that an IR band in this range may be due to a metal/support interaction.²³ Note the absence of any other IR bands above 2120 cm^{-1} in Figure 1, which indicates the absence of $\text{Cu}^{\delta+}$ sites on the surface.^{12,14,15} Some other weak IR bands (not shown) are detected at 1660 and 1430 cm^{-1} , in accord with the observations on a reduced 4.9% $\text{Cu}/\text{Al}_2\text{O}_3$ catalyst¹² which can be assigned to CO stabilized on Al_2O_3 as bidentate and noncoordinated carbonate species.¹² The increase in T_a to 320 K (Figure 1, spectrum b) does not change the intensity of the IR band of the L_0 species, but for higher temperatures a progressive decrease is recorded (spectra c-g) without any significant shift of the IR band which disappears at $T_a = 550$ K. Figure 2 compares the FTIR spectra at 300 K before heating to 550 K in 1% CO/He (spectrum a) and after cooling from 550 K in 1% CO/He (spectrum b). It can be observed that spectra a and b in Figure 2 are similar (slight

decrease by 5% in spectrum b), indicating that there are no strong modifications of the Cu particles in the course of the CO adsorption at high temperatures (it is shown below that the aging of the copper particles leads to different observations). This is the main difference compared to supported Pt^{8,10} and Pd¹¹ catalysts which led to the reconstruction and/or the poisoning (carbon deposition coming from the CO dissociation/disproportionation) of the metal particles in the course of the CO adsorption.

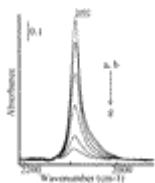


Figure 1 FTIR spectra recorded on the reduced 4.7% Cu/Al₂O₃ in the course of the CO adsorption at various temperatures with $P_a = 1000$ Pa: (a) 300 K; (b) 320 K; (c) 350 K; (d) 380 K; (e) 410 K; (f) 445 K; (g) 475 K.

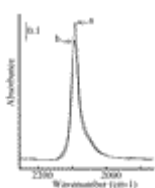


Figure 2 Comparison of the FTIR spectra of CO adsorbed at 300 K (1% CO/He) before and after heating at 550 K: (a) before and (b) after heating.

The change in the coverage θ of the Cu^o sites by the L₀ species in the presence of the 1% CO/He mixture as a function of T_a , can be obtained using the ratio $\theta = A/A_M$ with A the IR band area at T_a and A_M the highest IR band area (at 300 K) and assuming:^{8,10,11} (a) a linear relationship between the intensity of the IR band and the quantity of the linear CO species on the surface and (b) that the IR absorption extinction coefficient is independent of the adsorption temperature. Figure 3 shows (curve a) the evolution of θ with T_a using the spectra in Figure 1. The curve b which overlaps curve a, corresponds to the evolution of θ during the cooling step from 550 to 300 K and confirms that there are no modifications of the Cu surface during the CO adsorption at high temperatures.

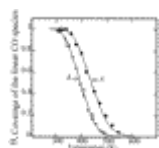


Figure 3 Evolution of the coverage of the L₀ species according to the adsorption temperature: +, (a) experimental data with $P_a = 10^3$ Pa; □, (b) experimental data with $P_a = 10^3$ Pa during the cooling to 300 K; ◆, (c) experimental data with $P_a = 10^4$ Pa; (d, e) theoretical coverage according to the adsorption model (see the text) with $E_1 = 57$ kJ/mol and $E_0 = 82$ kJ/mol, (d) $P_a = 10^3$ Pa and (e) $P_a = 10^4$ Pa.

Experiments similar to those described in Figure 1 have been performed with the 10% CO/He mixture on a fresh catalyst. The recorded spectra (not shown) are similar to those in Figure 1 with the same position and the same intensity of the IR band at 300 K. This last observation confirms the full coverage of the sites at 300 K even with the lowest CO partial pressure. Curve c in Figure 3 gives the evolution of the coverage of the L₀ species with T_a at $P_a = 10^4$ Pa. The profile of curve c is similar to that of curve a and as expected, for $T_a > 350$ K, θ is higher in curve c ($P_a = 10^4$ Pa) than in curve a ($P_a = 10^3$ Pa). Note that the coverage $\theta = 1$ is related to the saturation on the sites adsorbing the L₀ species between 300 and 550 K and not to the full coverage of the copper particles (monolayer) which is may be obtained by decreasing T_a and/or increasing P_a . This may explain the linear relationship between the

amount of L_0 species and the IR band area. In the discussion section, the curves $\theta = f(T_a)$ in Figure 3 are used for the determination of the Hs.A. of the L_0 species in the coverage range 0-1.

3.3. Adsorption of CO on the Oxidized Cu/Al₂O₃ Solid. Figure 4 shows the spectrum recorded after 30 s in 1% CO/He on the solid cooled in He after oxidation at 713 K (spectrum a). The IR band detected at 2120 cm⁻¹ can be assigned in agreement with the literature^{12,14,15,17,23} to a linear CO species (denoted by L_1) adsorbed on Cu⁺ sites. The exact position of the IR band in the range 2140-2110 cm⁻¹ is considered to be dependent on the environment of the Cu⁺ sites.^{14,17} Note the absence of IR bands above 2140 cm⁻¹ which are usually assigned to linear CO species on Cu²⁺ species.^{12,17} The intensity of the IR band at 2120 cm⁻¹ increases with time on stream as shown in spectrum b recorded after 10 min. The increase in T_a (15 K/min) up to 473 K followed by a cooling to 300 K in 1% CO/He leads to Figure 4c, which shows that the number of Cu⁺ sites has increased. It is shown below that Figure 4c corresponds to the maximum in the concentration of the L_1 species on the surface. Figure 4c has been obtained after the experiment leading to Figure 2a. The ratio between the IR band area A_{2120} (Figure 4c)/ A_{2090} (Figure 2a) is 1.5, in good accord with the ratio of the IR absorption extinction coefficients of the L_1 and L_0 species determined by Kohler et al. on Cu/SiO₂ catalysts: $\epsilon_{L1}/\epsilon_{L0} = 1.8$.²⁴ This means that there is around the same number of superficial sites for Cu⁺ and Cu^o. At moderate temperatures, Sadykov and Tikhov²⁴ considered that there was a reduction (CO or H₂ as reagents) of the surface of CuO particles (10-20% of the oxygen monolayer was removed) without the appearance of nuclei of any new phases. This interpretation agrees with the fact that the main peak in the course of the H₂ TPR starts around 473 K. It seems that the increase in intensity of the IR band of the L_1 species with the reduction temperature (Figure 4) corresponds to the only surface reduction of the copper oxide particles. The increase in the number of Cu⁺ sites in the course of the first heating in 1% CO/He does not allow us to follow, using this experiment, the evolution of the coverage of the L_1 species with T_a as done above for the L_0 species. This determination can be only performed after the surface reduction of the CuO particles with CO gives the maximum of the Cu⁺ sites on the surface. However, it must be take into account that (a) the experimental reduction conditions leading to the maximum of Cu⁺ on the surface are not well-defined and (b) at high temperatures, in the presence of CO, the number of Cu⁺ sites may decrease due to their deep reduction into Cu^o sites.

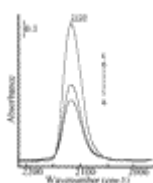


Figure 4 FTIR spectra on the oxidized Cu/Al₂O₃ in the course of the adsorption of 1% CO/He: (a) 0.5 min at 300 K; (b) 10 min at 300 K; (c) at 473 K.

The maximum of Cu⁺ sites on the surface has been obtained according to the following procedure: the 1% CO/He mixture is introduced at 300 K on the oxidized solid (Figure 4) and then the temperature is increased (15 K/min) to a final temperature T_f (formation of the Cu⁺ sites). Then the solid is cooled to room temperature in 1% CO/He and T_a is increased while the spectra are recorded periodically. If $T_f > 400$ K, the IR band area of the L_1 species is maximum at $T_a = 300$ K. The increase in T_a (spectra not shown) leads to the progressive decrease in intensity of the IR band without a significant shift. Curve a in Figure 5 shows the

evolution in the ratio (IR band area at T_a)/(IR band area at 300 K) for $T_f = 400$ K. It can be observed that (a) the ratio is initially constant and then decreases progressively until $T_a \approx 440$ K (section a_1), (b) between 440 and 490 K the ratio is constant (section a_2), and (c) above 490 K the ratio decreases (section a_3). The profile of curve a can be interpreted as follows: (a) section a_1 indicates the evolution of the coverage of the L_1 species on the Cu^+ sites formed after reduction at $T_f = 400$ K and its profile is similar to that observed in Figure 3 for the L_0 species; (b) section a_2 is due to two processes, the decrease in coverage of the Cu^+ sites with T_a and the increase in the number of Cu^+ sites by the reduction of the oxide surface for $T_a > T_f$; (c) section a_3 is probably due to the decrease in coverage of the Cu^+ sites with T_a and to the disappearance of Cu^+ sites by their deep reduction into Cu° . Note that the L_0 species cannot be detected in the temperature range of section a_3 because its coverage is very low as shown in Figure 3. Taking into account the processes involved in curve a, an experiment similar to that described above has been performed but with $T_f = 490$ K (the final temperature of section a_2) which may correspond to the maximum of the Cu^+ sites on the surface. There are several studies which indicate that the reduction of an oxidized supported copper catalyst to ≈ 450 K leads after adsorption of CO at 300 K to FTIR spectra with only the IR band of the L_1 while the IR band of the L_0 species is detected for a higher reduction temperature.^{12,18,24} Curve b in Figure 5 gives the evolution of the ratio (IR band area at T_a)/(IR band area at 300 K) for $T_f = 490$ K. This curve overlaps curve a in the range 300-440 K and then decreases progressively. In curve b, the absence of a section similar to section a_2 indicates that the reduction process leading to the Cu^+ sites was over at $T_f = 490$ K. Note that the profile of curve b in Figure 5 is similar to the curves $\theta = f(T_a)$ for the L_0 species in Figure 3. To facilitate the comparison, we have reported curve a in Figure 3 as curve c in Figure 4. Curve b can be considered as representative of the evolution of the coverage of the L_1 species with T_a . At high temperatures, however, the decrease in intensity of the IR band of the L_1 species may be due to the reduction of Cu^+ to Cu° and the coverage of the Cu^+ sites for $T_a > T_f$ is probably underestimated in curve b Figure 5. Corrected values of the coverages can be obtained by the evaluation of the contribution of the $\text{Cu}^+ \rightarrow \text{Cu}^\circ$ reduction to the decrease in the IR band of the L_1 species at high temperatures according to the following experiments.

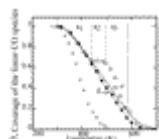


Figure 5 Evolution of the coverage of the L_1 species according to the adsorption temperature with $P_a = 10^3$ Pa: \square , (a) solid reduced in 1% CO/He at $T_f = 400$ K; \blacklozenge , (b) solid reduced in 1% CO/He at $T_f = 490$ K; \times , (c) coverage of the L_0 species; (d, e) theoretical coverage according to the adsorption model (see the text for more details).

The oxidized solid is partially reduced at 490 K in 1% CO/He as described above, and then after cooling to 300 K (Figure 4c) the adsorption temperature is increased to $T_{af} = 580$ K (Figure 6a) followed by a new cooling to 300 K in the presence of CO (Figure 6b). The lower intensity of spectrum b as compared to spectrum c in Figure 4 (decrease by 38%) is due to the reduction $\text{Cu}^+ \rightarrow \text{Cu}^\circ$ ($\epsilon_{L_0} < \epsilon_{L_1}$). This is in agreement with the profile of spectrum b in Figure 6, which shows a maximum at 2109 cm^{-1} (L_0 species) and a shoulder at $\approx 2125 \text{ cm}^{-1}$ (L_1 species). Figure 6c has been recorded after adsorption of CO at 300 K on the fully reduced catalyst (see Figure 1). The subtraction (spectrum b) - x (spectrum c) with x a factor to eliminate the IR band of the L_0 species leads to spectrum d, which represents the contribution of the L_1 species to spectrum b. The corrected coverage of the L_1 species at $T_{af} = 580$ K is given by $\theta_c = (\text{IR band area in Figure 6a})/(\text{IR band area in Figure 6d})$ and it is reported with the symbol \odot in Figure 5. The above procedure has been applied for different T_{af} values, and

the corresponding corrected coverages (symbol \odot) are reported in Figure 5. Note that (a) the above subtraction is easy because the positions of the IR bands are not significantly modified by the adsorption at high temperatures, (b) the formation of the Cu° sites at high temperatures does not impose a correction of the IR band area recorded at T_{af} (Figure 6a) because the coverage of the Cu° sites is very low for $T_{\text{af}} > 500$ K, and (c) for $T_{\text{af}} < 500$ K the IR bands recorded at 300 K before and after adsorption at T_{af} are identical. In the next section curve d in Figure 5 at low temperatures and the corrected coverages at high temperatures are used for the determination of the Hs.A. of the L_1 species on the Cu^+ sites.

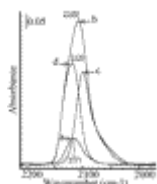


Figure 6 Treatment of the FTIR spectra for determination of the contributions of the L_0 and L_1 species: (a) in 1% CO/He at 580 K; (b) after cooling to 300 K after spectrum a; (c) at 300 K on the reduced solid; (d) after subtraction (spectrum b) - x (spectrum c).

4. Discussion

In the first part of the discussion we present the determination of the Hs.A. of the L_0 and L_1 species at various coverages as well as the comparison with the data in the literature. In the second part the influences of the modifications of the catalyst, aging and incomplete reduction on the Hs.A. of the two adsorbed species, are presented. In the final part of the discussion, it is shown that the values of the Hs.A. of the L_0 and L_1 species can be used to quantitatively interpret the literature data on the difference in the stability of the two species at 300 K during a desorption process.

4.1. Heats of Adsorption of the L_0 Species on the Cu° Sites as a Function of the Coverage. The curve a, $\theta = f(T_a)$ (Figure 3a) is very similar to those previously observed on supported $\text{Pt}^{8,10}$ and Pd^{11} catalysts. We have shown that this curve corresponds to an adsorption model which considers that the E_{θ} values linearly decrease with increase in θ ($E_{\theta} = E_0 - \alpha\theta$). This assumption provides an expression of the coverage as a function of the adsorption parameters^{8,10} (also see references therein):

$$\theta = \frac{RT_a}{\Delta E} \ln \left(\frac{1 + \lambda_0 P_a}{1 + \lambda_1 P_a} \right) \quad (1)$$

where ΔE is the difference in the Hs.A. at $\theta = 0$ (E_0) and $\theta = 1$ (E_1); λ_0 and λ_1 are the adsorption coefficients at $\theta = 0$ and $\theta = 1$. The Temkin equation^{4,5} is obtained assuming $(\lambda_0 P_a) \gg 1$ and $(\lambda_1 P_a) \ll 1$ in expression 2:

$$\theta = \frac{RT_a}{\Delta E} \ln(1 + \lambda_0 P_a) \quad (2)$$

Assuming an expression of the adsorption coefficient $\lambda_0 = A \exp(E_0/RT)$ (the preexponential factor A is assumed independent of T), expression 2 leads to

$$\theta = \left[\frac{R}{\Delta E} \ln(AP_a) \right] T_a + \frac{E_0}{\Delta E} \quad (3)$$

This shows that for a given value of P_a , θ varies with T_a according to a straight line (Temkin's approximations correspond to the linear fraction of the isobar as observed in Figure 3). Expression 3 shows that the extension of the linear section of the isobar must intercept the θ axis in $E_0/\Delta E$ at $T = 0$ K independently of P_a . This is shown in Figure 7 for $P_a = 10^3$ Pa and $P_a = 10^4$ Pa, and the interception point gives $E_0/\Delta E = 3.4 \pm 0.2$, which indicates that there is an important difference between E_0 and E_1 .

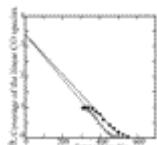


Figure 7 Comparison of the experimental values of the coverages of the L_0 species for $P_a = 10^3$ Pa (+) and $P_a = 10^4$ Pa (◆) with Temkin's equation showing $E_0/\Delta E$ at $T = 0$ K.

It can also be assumed as considered in previous studies^{8,10,11} that the L_0 species is immobile and that the adsorption coefficient is provided by the statistical thermodynamics assuming the loss of three degrees of translation:

$$\lambda = \frac{h^3}{k(2\pi mk)^{3/2}} \frac{1}{T_a^{5/2}} \exp\left(\frac{E_d - E_a}{RT_a}\right) \quad (4)$$

where h is Planck's constant, k is Boltzmann's constant, m is the weight of the molecule (28×10^{-3} kg/ 6.02×10^{23}), E_d and E_a are the activation energies of desorption and adsorption, respectively, and $E_d - E_a$ is the H.A. Expression 4 provides a preexponential factor of 2.9×10^{-13} Pa⁻¹ at 600 K. Considering expression 3, it can be observed that the slope of the straight line in Figure 7 enables the determination of ΔE assuming $A = 2.9 \times 10^{-13}$ Pa⁻¹: $\Delta E = 25$ kJ/mol. This leads to $E_0 = 3.4 \times 25 = 85$ kJ/mol and $E_1 = 60$ kJ/mol with an accuracy of ± 5 kJ/mol.

The above E_1 and E_0 values are obtained using Temkin's approximations. However, as achieved previously on supported Pt^{8,10} and Pd¹¹ catalysts, E_0 and E_1 can be determined without these approximations considering (a) the experimental curve a in Figure 3, (b) the theoretical coverage provided by expression 1 (with $P = 10^3$ Pa), and (c) the adsorption coefficient of expression 4. It is only required that we find E_1 and E_0 leading to a theoretical curve $\theta = f(T_a)$ in agreement with the experimental data. Curve d in Figure 3 is obtained using $E_1 = 57$ kJ/mol and $E_0 = 82$ kJ/mol. Note that (a) E_1 and E_0 lead to $E_0/\Delta E = 82/(82 - 57) = 3.28$ in agreement with 3.4 determined above with expression 3, and (b) the determination of $E\theta$ using the above procedure is very accurate because modification of a few kJ/mol (≤ 5 kJ/mol) of E_0 or/and E_1 leads to a theoretical curve significantly different from the experimental data. Curve e in Figure 3 is obtained using in expression 1 $P_a = 10^4$ Pa with $E_1 = 57$ kJ/mol and $E_0 = 82$ kJ/mol. The very good agreement between the adsorption model and the experimental data for the two adsorption pressures can be observed.

As achieved previously with a Pt/Al₂O₃ catalyst,¹⁰ the Hs.A. of the L_0 species obtained by the above adsorption model can be compared to the isosteric Hs.A. using the two isobars at 10^3 Pa and 10^4 Pa (curves a and c in Figure 3) and the Clausius-Clapeyron equation:

$$\left. \frac{d(\ln P_a)}{d(1/T_a)} \right|_{\theta} = \frac{-\Delta H_{\theta}}{R} \quad (5)$$

The interest in the comparison is that the procedure using the adsorption model assumes that the adsorption coefficient is given by statistical thermodynamics considering an immobile adsorbed species, while this assumption is not necessary using the Clausius-Clapeyron equation. Curve a in Figure 8 gives the evolution of the isosteric Hs.A. in the coverage range 0.9-0.1. The isosteric Hs.A. $\Delta H_0 = 88$ kJ/mol and $\Delta H_1 = 56$ kJ/mol at $\theta = 0$ and $\theta = 1$, respectively, are extrapolated from curve a. These values are in very good agreement with E_0 and E_1 found above, and this validates the different assumptions involved in the adsorption model, in particular those linked to expression 4. Moreover, the profile of curve a in Figure 8 is in agreement with the assumption on the linear decrease in the H.A. with increase in θ considered in the adsorption model.

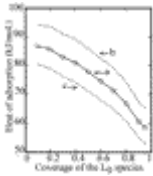


Figure 8 Isosteric heats of adsorption of the L_0 species as a function of the coverage: (a) using the experimental curves a and c in Figure 3; (b, c) values assuming $T_a + 2$ K and $T_a - 2$ K (see the text for more details).

4.2 Heats of Adsorption of the L_1 Species on the Cu^+ Sites as a Function of the Coverage.

The above procedure can be used for the determination of the Hs.A. of the L_1 species (denoted by E') using the experimental curve b in Figure 5. Considering the linear section of the curve b and expression 3, it is found that $E'_0/\Delta E' = 2.2$ (interception point at $T = 0$ K). The experimental slope of this section and expression 3 leads to $\Delta E' = 50.7$ kJ/mol, and assuming $A = 2.9 \times 10^{-13}$ Pa $^{-1}$, it is found that $E'_0 = 50.7 \times 2.2 \approx 112$ kJ/mol and $E'_1 = 61$ kJ/mol. As described above, expressions 1 (without Temkin's approximation) and 4 can be used to fit the experimental curve b. Curve d in Figure 5 is obtained using $E'_0 = 110$ kJ/mol and $E'_1 = 58$ kJ/mol. We have shown above that the values of the coverage in curve b at high temperatures are underestimated and that the corrected coverage (symbol \odot) must be used. This leads to the following values: $E'_0/\Delta E' = 2.15$, $\Delta E' = 53.7$, $E'_0 = 115$ kJ/mol, and $E'_1 = 61.4$ kJ/mol. Finally curve e is obtained with $E'_0 = 115$ kJ/mol and $E'_1 = 58$ kJ/mol. Note that we have not presented, for the L_1 species, the results with the 10% CO/He mixture because the reduction processes to obtain the maximum of Cu^+ as described in Figure 5 and to reduce Cu^+ into Cu° are significantly modified as compared to the 1% CO/He mixture. This shows one of the interests of the procedure using the adsorption model (a single isobar) compared to an isosteric method (at least two isobars) to measure the Hs.A. of an adsorbed species on sites (Cu^+) which may change (amount in the present study) with the adsorption conditions.

The above values of the H.A. for the L_0 species ($E_0 = 82$ kJ/mol at $\theta = 0$ to $E_1 = 57$ kJ/mol at $\theta = 1$) and for the L_1 species ($E'_0 = 115$ kJ/mol at $\theta = 0$ to $E'_1 = 58$ kJ/mol at $\theta = 1$) are compared in the following section to the data in the literature on copper-containing solids before the presentation of other results such as the effects of the aging of the catalyst and the simultaneous presence of Cu° and Cu^+ sites (incomplete reduction of the copper particles) on the Hs.A.

4.3. Comparison of the Hs.A. of the L₀ and L₁ Species with the Data in the Literature.

There is an agreement in the literature to consider that the H.A. of CO on Cu⁺ sites is higher than that on Cu⁰.^{12,26} This is an argument to explain the disappearance of the IR band of L₀ species during a desorption at 300 K while the intensity of the IR band of the L₁ species decreases in the first stage of the desorption and then is constant.¹⁸ The results of the present study confirm this conclusion: E_{θ} is higher than E_{θ} whatever θ , but in addition it is shown that the difference is very small at high coverages ($E_1 - E_0 \approx 1-2$ kJ/mol) and increases with decrease in coverage ($E'_0 - E_0 \approx 30$ kJ/mol). Dandekar and Vannice¹² reported various data from the literature on the Hs.A. of CO on Cu⁰ and Cu⁺ for different Cu-containing solids (see Table 4 in ref 12). For a given oxidation state of Cu it was observed that there were some significant differences from one study to another. For instance, considering Cu⁰ the Hs.A. were in the range 18 kJ/mol on Cu/ γ -Al₂O₃¹² to 60 kJ/mol on Cu(100),²⁷ Cu(110),²⁸ and 6.6% Cu/SiO₂.²⁹ Similarly considering Cu⁺, the Hs.A. were in the range 22 kJ/mol on Cu/SiO₂³⁰ to 84 kJ/mol on a Cu₂O film.³¹ The discrepancy between the studies can be due to the effects of various parameters such as the exposed face, the particle size, and the nature of the support. However, the above comparison¹² did not indicate the coverage associated with the H.A. values, and this may explain some discrepancies. For instance, the H.A. of the L₁ species was 41 kJ/mol on Cu/ γ -Al₂O₃¹² at high coverage and 87 kJ/mol at $\theta = 0.09$ on Cu₂O(100).³² In that sense, Cox and Schultz²⁶ reported the data of the literature at low coverages (see Table 1 in ref 26), and they observed that for Cu⁺ sites the Hs.A. of CO on different Cu-containing solids were in a short range of values, 70-87 kJ/mol, with an accuracy of ± 9 kJ/mol. The discrepancy between the various studies can also be due to the inconvenience of the analytical methods used for the determination of the H.A.: isosteric and calorimetric (average of several species) and TPD (values of the frequency factor). In the comparison presented below involving different Cu-containing solids, we present the Hs.A. of the L₀ and L₁ species at low coverages and then we discuss the profiles of the curves Hs.A. = $f(\theta)$.

The Hs.A. of CO at low coverage on Cu single crystals varied slightly with the exposed face from $\approx 60 \pm 2$ kJ/mol on Cu(100),²⁷ Cu(110),³³⁻³⁵ Cu(211), and Cu(311)¹³ to ≈ 52 kJ/mol on Cu(111).^{36,37} Some studies report higher values of $\approx 70 \pm 2$ kJ/mol on Cu(100) at $\theta < 0.1$ ^{22,38} and on a Cu film.³⁹ It appears that $E_0 = 82$ kJ/mol found in the present study is slightly higher than those in the literature on single crystals which are in the range 60-70 kJ/mol. This may be related to a particle size or a support effect, but it can be also due to the fact that at the difference of several of the aforementioned studies we use adsorption equilibrium conditions at high pressures and temperatures. Another result of the present study is that the Hs.A. of the L₀ species linearly decrease with increase in coverage from $E_0 = 82$ kJ/mol to $E_1 = 57$ kJ/mol. If there is an agreement to consider that qualitatively the Hs.A. of the L₀ species decrease with increase in coverage, there are very few studies on a quantitative determination. Papp and Pritchard¹³ indicated that on Cu(311) the H.A. was constant at low coverage (< 0.4 L, L = langmuir) and then linearly decreased from 61 to 20 kJ/mol at 1 L. On Cu(100), Truong et al.²² indicated that the Hs.A. decreased with coverage from 70 kJ/mol at $\theta = 0$ to 52 kJ/mol at $\theta = 0.35$ according to a profile slightly different from a straight line. Their results were in accord with an early work³⁸ which indicated a decrease from 70 to 48 kJ/mol at $\theta = 0.5$. It must be noted that the isosteric method is very sensitive to the experimental uncertainties on T_a . For instance, curves b and c in Figure 8 give the isosteric Hs.A. using the Clausius-Clapeyron equation considering for curve b $T_a + 2$ K for the isobar $P_a = 10^3$ Pa (curve a in Figure 3) and $T_a - 2$ K for the isobar $P_a = 10^4$ Pa (curve c in Figure 3) and for curve c $T_a - 2$ K for the isobar $P_a = 10^3$ Pa and $T_a + 2$ K for the isobar $P_a = 10^4$ Pa. Figure 8 shows that the experimental uncertainties on T_a may lead to various profiles for the curves $\Delta H = f(\theta)$ between the two curves b and c.

There are only a few studies on the Hs.A. of CO on reduced supported copper catalysts. Bandekar and Vannice,¹² assuming Langmuir's adsorption model, determined 17 kJ/mol for the L₀ species at low coverages on Cu/SiO₂ and Cu/Al₂O₃ catalysts. The authors¹² considered that this low value was perhaps due to an incomplete reduction of copper. Note that in the present study the catalyst is fully reduced (absence of IR band of CO adsorbed on Cu⁺ and Cu²⁺) and this may explain that E₀ is similar to the values determined on single crystals and significantly higher than in ref 12. Kohler et al.²⁴ have determined, using FTIR spectra and the isosteric method, the Hs.A. of CO on reduced Cu/SiO₂ catalysts with different copper loadings in the range 2.1-9.5 wt %. They observed that the Hs.A. at low coverage increased with the copper loading from ≈30 kJ/mol for 2.1% to ≈55 kJ/mol for 9.5%. This was attributed to a particle size effect²⁴ considering that the diameter of the particles changed from <2 nm for 2.1% Cu/SiO₂ to ≈5 nm for 9.5% Cu/SiO₂. Moreover, for the different solids it was observed that the Hs.A. decreased with increase in θ to a common value (22 kJ/mol at θ = 1) according to Freundlich's adsorption model.²⁴ Monti et al.²⁹ on a reduced 6.6% Cu/SiO₂ catalyst determined 60 ± 5 kJ/mol using FTIR spectroscopy (CO/H₂ mixture, IR band at 2117 cm⁻¹) and assuming Langmuir's model. This value is not very different from the average value (E₀ + E₁)/2 ≈70 kJ/mol of the present study. Finally, it appears that the H.A. of the L₀ species at low coverage found in the present study is higher than the values found in the literature on reduced supported copper catalysts. This may be due to different effects, in particular the particle size²⁴ (low dispersion of the present catalyst) and/or the incomplete reduction of the copper oxide.¹²

For the Hs.A. of CO on Cu⁺ sites a theoretical model⁴⁰ on a Cu/ZnO system led to 93.4 kJ/mol in good accord with E'₀ = 115 kJ/mol. Moreover, on Cu₂O/ZnO⁴¹ it has been determined (microcalorimetry) that there was a site energy distribution with a peak at ≈80 kJ/mol but with a substantial fraction of sites having a H.A. higher than 120 kJ/mol. On Cu₂O (100), Cox and Schulz have determined 70 kJ/mol at low coverage by TPD (ν = 10¹³ s⁻¹), while Stone et al. using a calorimetric method indicated 84 kJ/mol on Cu₂O film³¹ and 87 kJ/mol at θ = 0.09 and 75 kJ/mol at θ = 0.26 on Cu₂O powder.⁴² On Cu₂O/Al₂O₃ a value of 71 kJ/mol was reported⁴³ while on CuY zeolite Huang⁴⁴ determined ≈60 kJ/mol in the θ range 0-1. In the high coverage range and assuming Langmuir's model, Dandekar and Vannice¹² found 55 kJ/mol on Cu/SiO₂, 41 kJ/mol on Cu/Al₂O₃, and 51 kJ/mol on Cu deposited on a synthetic diamond powder. These values are in good accord with E'₁ = 57 kJ/mol. Taking into account the difference in the solids and the analytical methods involved in the above comparison on CO adsorbed on Cu⁺, it can be considered that the values found in the present study are slightly higher at low coverage (by ≈20 kJ/mol) as compared to several studies and in good agreement with the results of ref 12 at high coverages. Some studies report significantly lower values for the H.A. of CO on Cu⁺, 30 kJ/mol on Cu/Al₂O₃⁴⁵ and 21 kJ/mol on Cu/SiO₂,³⁰ but in the two cases the values are obtained from the rate expression of a catalytic reaction involving several constants and this procedure is subjected to significant uncertainties. Moreover, Kohler et al.²⁴ have shown that the H.A. of CO on Cu²⁺ sites of a Cu/SiO₂ catalyst was 29 kJ/mol, in accord with recent results on Cu/Al₂O₃.¹² If Cu⁺ and Cu²⁺ sites are present on an oxidized catalyst, it can be understood that analytical methods (i.e., microcalorimetry) which do not enable to evaluate the contribution of each species (as in the present study) to the Hs.A. may lead to an underestimation of the Hs.A. of the L₁ species.

There are various effects which can be evoked to explain the differences noted above in the H.A. of CO for a given oxidation number of Cu (Cu⁰ and Cu⁺) such as the particle size²⁴ and the incomplete reduction of the copper oxide particles.¹² In the following part of the

discussion the influence of these parameters on the Hs.A. of the L_0 and L_1 species is presented.

4.4. Effect of the Aging of the Catalyst on the Heats of Adsorption of CO. The same pellet of catalyst was used for several experiments, and we have observed a strong decrease in intensity of the IR band of the L_0 species alongside a shift to higher wavenumbers after several cycles of pretreatment/adsorption of CO at high temperatures. For instance, Figure 9 compares the IR bands observed on a reduced catalyst after the first pretreatment (spectrum a) and after 10 cycles (spectrum b). It can be observed that (a) the IR band shifts from 2092 to 2102 cm^{-1} and (b) the intensity is strongly decreased (by 50%). This can be related to a sintering of the copper particles (decrease in intensity of the IR band) in the course of the various treatments and to a modification of the surface structure considering the shift in the IR band.^{15,18,19} The evolution of the coverage of the L_0 species adsorbed on the aged solid with the 1% CO/He mixture and according to the procedure used for the fresh catalyst is indicated in curve a of Figure 10. This curve overlaps curve b in Figure 10 observed with a fresh catalyst, and this leads to the conclusion that there is no modification of the Hs.A. of the L_0 species either with the sintering of the reduced copper particles (particle size effect) and/or with the modification of the surface structure. This last point is in accord with the results on single crystals which show that the Hs.A. are only slightly affected by the exposed face. However, this conclusion is not in contradiction with that of Kohler et al.,²⁴ who observed a particle size effect because this effect is probably associated with a high dispersion of the copper particles in the range 2-5 nm, while the dispersion of the present catalyst indicates larger particles ($d \approx 10$ nm) using the equation¹² $d(\text{nm}) = 1.1/D$.

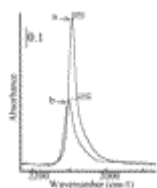


Figure 9 Modifications of the FTIR spectra of the L_0 species on the reduced $\text{Cu}/\text{Al}_2\text{O}_3$ solid: (a) fresh solid; (b) aged solid.

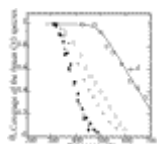


Figure 10 Coverage of the adsorbed species on the $\text{Cu}/\text{Al}_2\text{O}_3$ solid after various pretreatments: \times , (a) L_0 on the aged reduced solid, \blacklozenge , (b) L_0 on the fresh reduced solid; \square , (c) bridged CO species on the aged solid; \square , (d) theoretical coverage of the bridged CO species according to the adsorption model; \cdot , (e) L_0 species in the presence of the L_1 species; $+$, (f) L_1 species in the presence of the L_0 ; \circ , (g) L_1 species in the absence of the L_0 species.

The reduced aged catalyst leads to significant differences as compared with a fresh catalyst for the 10% CO/He mixture as shown Figure 11. Spectrum a recorded after 0.5 min is similar to the spectrum recorded with the 1% CO/He mixture (IR band at 2102 cm^{-1} , L_0 species). However, with time on stream a decrease in intensity of this IR band alongside the appearance of shoulders at low wavenumbers (Figure 11b) which are clearly discerned at 2043, 2010, and 1943 cm^{-1} after 11 min (Figure 11c) is observed. These observations indicate that the Cu° sites are slowly converted into other sites which differently adsorb CO. This restructuring of the copper surface develops with increase in T_a , and this leads to the disappearance of the shoulder at 2043 cm^{-1} (Figure 11d, $T = 380$ K) while the shoulder at 2010 cm^{-1} increases and is detected as a distinct IR band (Figure 11d-f). The decrease in intensity of the main IR band at 2100 cm^{-1} is due to two processes: the transformation of the sites as observed at 300 K and

the decrease in coverage of the remaining sites. Note that the intensities of the IR band at 2010 cm^{-1} and of the shoulder at 1943 cm^{-1} are constant between 424 and 473 K (Figure 11e,f). For $T_a > 473\text{ K}$ it is observed that the shoulder at 1943 cm^{-1} decreases and disappears at 550 K (Figure 12a-c) and only the IR band at 2002 cm^{-1} is detected. This IR band slowly decreases with increase in T_a (Figure 12d-f) and shifts to lower wavenumbers (1994 cm^{-1} at 616 K, 1983 cm^{-1} at 713 K, and 1978 cm^{-1} at 748 K). The spectrum recorded at 458 K after cooling from 748 K (Figure 12g) shows that there are no strong modifications of the IR band at 2002 cm^{-1} (the shoulder 1943 cm^{-1} is not detected after cooling). An IR band at $\approx 2000\text{ cm}^{-1}$ after adsorption of CO on copper-containing solids is rarely mentioned in the literature. Dandekar and Vannice¹² assigned an IR band at 2003 cm^{-1} observed on a reduced (H_2 , 573 K) 4.9% Cu/ Al_2O_3 solid to a bridged CO species on Cu^\ominus sites. On a reduced (H_2 , 723 K) Cu/ $\text{CeO}_2/\text{Al}_2\text{O}_3$ catalyst an IR band at 2000 cm^{-1} was ascribed to CO adsorbed at the copper particle/support interface.⁴⁶ On the present catalyst, whatever T_a , the IR band is observed neither on the fresh catalyst nor on the aged solid with 1% CO/He. This seems against the interpretation involving an interface particle/support, and we adopt the assignment of ref 12 (bridged CO species on Cu^\ominus , denoted by B). However, considering that the 2003 cm^{-1} IR band appears slowly at room temperature and increases during the heating in 10% CO/He, we assume that the sites are formed in the course of the adsorption of CO by the restructuring of the large copper particles formed by the aging of the catalyst (this restructuring is not observed on the fresh solid). Similarly the shoulder at 1943 cm^{-1} is attributed to another B species. This restructuring leads to a decrease in the number of Cu^\ominus sites forming the L_0 species (Figure 11). The shoulder at 2043 cm^{-1} is probably linked to Cu^\ominus sites formed in the course of the restructuring. For instance, an IR band at 2071 cm^{-1} is assigned to CO adsorbed at the border of small copper particles.¹⁵ Note that the restructuring of the copper surface is not accompanied by IR bands above 2100 cm^{-1} , indicating that there is no oxidation (considering for instance the dissociation of CO) of the reduced copper surface during the process. The results in Figure 12 can be used for the determination of the Hs.A. of the B species according to a procedure similar to that described for the L_0 and L_1 species with $\theta = A/A_m$ (A = the IR band area at T_a and A_m the highest IR band area measured at $T_a = 460\text{ K}$). Curve c in Figure 10 gives the evolution of the coverage of this species above $T_a = 450\text{ K}$. Curve d in Figure 10 is obtained using in expressions 1 and 4 $E_0 = 130\text{ kJ/mol}$ and $E_1 = 78\text{ kJ/mol}$ at $\theta = 0$ and $\theta = 1$, respectively. The good agreement between the experimental data and the adsorption model can be observed. Note that the B species formed on the reduced copper particles has Hs.A. strongly higher than those of the L_0 and L_1 species. We have found no data in the literature on similar values for the adsorption of CO on Cu-containing solids.

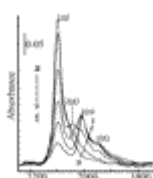


Figure 11 FTIR spectra recorded on the aged reduced Cu/ Al_2O_3 solid in the course of the CO adsorption with $P_a = 10^4\text{ Pa}$: (a-c) $T_a = 300\text{ K}$ and (a) $t = 0.5$ min, (b) 2.5, and (c) 11 min; (d) $T_a = 380\text{ K}$; (e) $T_a = 424\text{ K}$; (f) $T_a = 473\text{ K}$.

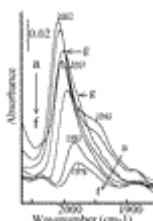


Figure 12 FTIR spectra recorded on the aged reduced Cu/ Al_2O_3 solid in the course of the CO adsorption with $P_a = 10^4\text{ Pa}$ at several adsorption temperatures: (a) 473 K; (b) 498 K; (c) 550 K; (d) 616 K; (e) 713 K; (f) 748 K; (g) at 458 K after cooling from 748 K.

For the L_1 species the position of its IR band is not modified (2120 cm^{-1}) by the aging of the catalyst and the curve $\theta = f(T_a)$ (not shown) overlaps that observed with the fresh solid.

4.5. Heat of Adsorption of L_0 and L_1 on the Partially Reduced $\text{Cu}/\text{Al}_2\text{O}_3$ Solid. We have shown above (Figure 6) that the treatment of the oxidized solid in 1% CO/He at $T > 500\text{ K}$ leads to the reduction of the Cu^+ sites into Cu^\ominus sites and at 300 K the FTIR spectrum indicates the presence of the two linear CO species L_0 and L_1 . The Hs.A. of the L_0 species in the presence of the L_1 species can be determined according to the following experiments. The 1% CO/He mixture is introduced at 300 K on the oxidized aged $\text{Cu}/\text{Al}_2\text{O}_3$ solid, and the temperature is increased up to $T_f = 620\text{ K}$. Then the solid is cooled to 300 K, leading to Figure 13a, which indicates the simultaneous presence of the L_1 species (shoulder at $\approx 2129\text{ cm}^{-1}$) and of the L_0 species (IR band at 2109 cm^{-1}). The temperature T_a is again increased to 563 K while the FTIR spectra are recorded periodically (Figure 13b-e). Note that after 490 K only the IR band of the L_1 species is detected. Finally, the catalyst is cooled to 300 K (Figure 13f), and by comparison with spectrum a it can be considered that the surface is not modified during the adsorption at 563 K. We have presented in Figure 6 the procedure for the determination of the contribution of the L_0 and L_1 species to the IR band observed in Figure 13a. The same procedure can be applied for the spectra in Figure 13 because there is no significant shift of the IR band of the L_0 and L_1 species with the adsorption temperature. This allows the determination of the evolution with T_a of the coverage of the L_0 species on a partially reduced catalyst as shown by curve e in Figure 10. It can be observed that curve e overlaps curve a for a fully reduced solid and this leads to the conclusion that the Hs.A. of the L_0 species on the Cu^\ominus sites are not modified by the presence of the L_1 species on the Cu^+ sites. Similarly, the coverage of the L_1 species in the presence of the L_0 species can be determined as shown by curve f in Figure 10. This curve is slightly lower in particular at low T_a than that observed in the absence of Cu^\ominus sites on the surface. Using expressions 1 and 4, it is found that curve f leads to $E'_0 = 98$ and $E'_1 = 58\text{ kJ/mol}$. E'_0 is slightly lower than the value found in the absence of Cu^\ominus sites (115 kJ/mol). Note that the absence of significant differences in the Hs.A. of the L_0 and L_1 species with the surface state is perhaps due to the reduction process of the copper fraction of the catalyst. For instance, it can be considered that the small particles are reduced before the large particles, leading to a situation where small reduced copper particles and large copper oxide particles coexist on the surface without any interactions.

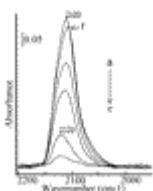


Figure 13 FTIR spectra recorded on a partially reduced (1% CO/He, $T_f = 620\text{ K}$) $\text{Cu}/\text{Al}_2\text{O}_3$ solid in the course of the CO adsorption with $P_a = 10^3\text{ Pa}$ at several adsorption temperatures: (a) 300 K; (b) 370 K; (c) 410 K; (d) 490 K, (e) 563 K; (f) at 300 K after cooling from 563 K.

4.6. Heats of Adsorption and Stability of the L_0 and L_1 Species during Desorption at 300 K. After adsorption of CO on copper-containing solids, it is common to ascertain the assignment of an IR band in the range $2130\text{--}2090\text{ cm}^{-1}$ to either the L_0 or the L_1 species by considering the stability of the IR band in the course of the desorption at 300 K. If the IR band disappears after few minutes, Cu^\ominus sites are involved (L_0 species), while if the IR band decreases but is still detected with a high intensity after several minutes, Cu^+ sites are

involved (L_1 species). For instance, Balkenende et al.¹⁸ on a Cu/SiO₂ catalyst indicated that the IR band of the L_0 species (≈ 2095 cm⁻¹) decreased to less than 2% of its initial intensity after evacuation of the gas phase while the IR band of the L_1 species (≈ 2120 cm⁻¹) decreases rapidly by 15% in about 5 min and a prolonged evacuation (1 h) caused a slow further decrease of 10%. We have observed similar results on the present Cu/Al₂O₃ solid during a desorption in He (600 cm³/min) at 300 K. The IR band of the L_0 species decreases rapidly leading to a coverage of 0.22 after 2 min and disappears after 6 min in He, while the IR band of the L_1 species also decreases rapidly leading to a coverage of 0.72 after 2 min and then more slowly to lead to an almost constant coverage $\theta = 0.53$ after 10 min.

The above observations can be quantified considering a first kinetic order for the desorption of the L_0 and L_1 species:

$$\frac{-d\theta}{dt} = \frac{kT}{h} \exp\left(-\frac{E_d(\theta)}{RT}\right)\theta \quad (6)$$

where $E_d(\theta)$ is the activation energy of desorption at θ assumed equal to the Hs.A. considering that the adsorption of the L_0 and L_1 species is not activated. Expression 6 can be used for the determination of the evolution of the coverage with the time of desorption of the L_0 species considering that the activation energy of desorption linearly varies from 57 kJ/mol at $\theta = 1$ to 82 kJ/mol at $\theta = 0$. This indicates that the coverage decreases to 0 after 6 min of desorption in agreement with the experimental observations. Expression 6 also allows the determination of the evolution of the coverage of the L_1 species in the course of a desorption considering that the activation energy of desorption linearly varies from 57 kJ/mol at $\theta = 1$ to 115 kJ/mol at $\theta = 0$. It is determined that the coverage rapidly decreases to 0.5 in the first minute and then tends to a constant value of around 0.38 after 10 min. Note that this result cannot be found assuming a constant heat of adsorption. The value of the coverage after more than 10 min of desorption ($\theta = 0.38$) is smaller than that determined experimentally ($\theta = 0.53$). This maybe due either to the fact that it is difficult during a desorption process to prevent the diffusion and readsorption processes^{1,11} or to a slight underestimation of the Hs.A. of the L_1 species due to the difficulty in the determination of θ at high temperatures linked to the deep reduction of the Cu⁺ sites (see the procedure for the determination of the coverage). For instance, to obtain a coverage limit of 0.53, it must be considered that the Hs.A. of the L_1 species are 65 kJ/mol at $\theta = 1$ and 125 kJ/mol at $\theta = 0$.

5. Conclusions

This study of the adsorption of CO on a 4.7% Cu/Al₂O₃ catalyst has shown that the IR spectra of the adsorbed species recorded at the adsorption equilibrium conditions ($P_a = 10^3$ Pa and 10^4 Pa, T_a in the range 300-720 K) can be used for the determination of the evolution with T_a of the coverage θ of two linear CO species adsorbed either on the Cu⁰ sites (2100-2090 cm⁻¹, L_0 species) of the fully reduced solid or on the Cu⁺ sites (2120 cm⁻¹, L_1 species) of a slightly reduced solid. The two curves $\theta = f(T_a)$ allows the determination of the Hs.A., E_θ , of the two species using an adsorption model which considers (a) a linear decrease in E_θ with increase in θ and (b) an immobile adsorbed species. The Hs.A. of the L_0 species vary with the coverage from $E_0 = 82$ kJ/mol at $\theta = 0$ to $E_1 = 57$ kJ/mol at $\theta = 1$, and the Hs.A. of the L_1 species vary with the coverage from $E'_0 = 115$ kJ/mol at $\theta = 0$ to $E'_1 = 58$ kJ/mol at $\theta = 1$. These values are not significantly modified by the aging of the catalyst and by the simultaneous presence of the L_0 and L_1 species on the surface. On an aged solid, a third CO species is detected leading to a IR band at 2010 cm⁻¹ at $T_a = 380$ K attributed to a bridged CO species. The Hs.A. of this

species are significantly higher than those of the L₀ and L₁ species and vary linearly with the coverage from 130 kJ/mol at $\theta=0$ to 78 kJ/mol at $\theta=1$.

Acknowledgment

We acknowledge with pleasure the FAURECIA Co., Bois sur Pré, 25 550 Bavans, France, for its financial support.

* To whom correspondence should be addressed. E-mail: Daniel.Bianchi@univ-lyon1.fr.

1. Demmin, R. A.; Gorte, R. J. *J. Catal.* **1984**, *90*, 32.[\[ChemPort\]](#)
2. Cardona-Martinez, N.; Dumesic, J. A. *Adv. Catal.* **1992**, *38*, 149.[\[ChemPort\]](#)
3. Sen, B.; Vannice, M. A. *J. Catal.* **1991**, *130*, 9.[\[ChemPort\]](#)
4. Tompkins, F. C. *Chemisorption of Gases on Metal*; Academic Press: London, 1978.
5. Clark, A. *The Theory of Adsorption and Catalysis*; Academic Press: London, 1970.
6. Kuhn, W. K.; Szanyi, J.; Goodman, D. W. *Surf. Sci.* **1994**, *303*, 377.[\[ChemPort\]](#)
7. Kuhn, W. K.; Szanyi, J.; Goodman, D. W. *Surf. Sci.* **1992**, *274*, L611.[\[ChemPort\]](#)
8. Chafik, T.; Dulaurent, O.; Gass, J. L.; Bianchi, D. *J. Catal.* **1998**, *179*, 503.[\[ChemPort\]](#)
9. Chafik, T.; Efstathiou, A. M.; Verykios, X. E. *J. Phys. Chem. B* **1997**, *101*, 7969.
10. Dulaurent, O.; Bianchi, D. *Appl. Catal., A* **2000**, *196*, 271.[\[ChemPort\]](#)
11. Dulaurent, O.; Chandes, K.; Bouly, C.; Bianchi, D. *J. Catal.* **1999**, *188*, 237.[\[ChemPort\]](#)
12. Dandekar, A.; Vannice, M. A. *J. Catal.* **1998**, *178*, 621.[\[ChemPort\]](#)
13. Papp, H.; Pritchard, J. *Surf. Sci.* **1975**, *53*, 371.[\[ChemPort\]](#)
14. Praliaud, H.; Mikhailenko, S.; Chajar, Z.; Primet, M. *Appl. Catal. B* **1998**, *16*, 359.[\[ChemPort\]](#)
15. Boccuzzi, F.; Chiorino, A.; Martra, G.; Gargano, M.; Ravasio, N.; Carrozzini, B. *J. Catal.* **1997**, *165*, 129.[\[ChemPort\]](#)
16. Martinez-Arias, A.; Fernandez-Garci, M.; Soria, J.; Conesa, J. C. *J. Catal.* **1999**, *182*, 367.[\[ChemPort\]](#)
17. Padley, M. B.; Rochester, C. H.; Hutchings, G. J.; King, F. *J. Catal.* **1994**, *148*, 438.[\[ChemPort\]](#)
18. Balkenende, A. R.; van Des Grift, C. J. G.; Meulenkaamp, E. A.; Geus, J. W. *Appl. Surf. Sci.* **1993**, *68*, 161 [\[ChemPort\]](#)

19. de Jong, K. P.; Geus, J. W.; Joziassse, J. *Appl. Surf. Sci.* **1980**, *6*, 273. [\[ChemPort\]](#)
20. Hollins, P.; Pritchard, J. In *Vibrational Spectroscopies for Adsorbed Species*; Bell, A. T., Hair, M. L., Eds.; ACS Symposium Series; American Chemical Society: Washington, DC, 1979; p 51.
21. Moskovits, M.; Hulse, J. E. *J. Phys. Chem.* **1977**, *61*, 2004.
22. Truong, C. M.; Rodriguez, J. A.; Goodman, D. W. *Surf. Sci. Lett.* **1992**, *271*, L385. [\[ChemPort\]](#)
23. Martinez-Arias, A.; Cataluna, R.; Conesa, J. C.; Soria, J. *J. Phys. Chem. B* **1998**, *102*, 809. [\[Full text - ACS\]](#) [\[ChemPort\]](#)
24. Kohler, M. A.; Cant, N. W.; Wainwright M. S.; Trim, D. L. *J. Catal.* **1989**, *117*, 188. [\[ChemPort\]](#)
25. Sadykov, V. A.; Tikhov, S. F. *J. Catal.* **1997**, *165*, 279. [\[ChemPort\]](#)
26. Cox, D. F.; Schulz, K. H. *Surf. Sci.* **1991**, *249*, 138. [\[ChemPort\]](#)
27. Pritchard, J. *J. Vac. Sci. Technol.* **1971**, *9*, 895.
28. Ahner, J.; Mocuta, D.; Ramsier, R. D.; Yates, J. T., Jr. *J. Chem. Phys.* **1996**, *105*, 6553. [\[ChemPort\]](#)
29. Monti, D. M.; Cant, N. W.; Trimm, D. L.; Wainwright, M. S. *J. Catal.* **1986**, *100*, 17. [\[ChemPort\]](#)
30. London, J. W.; Bell, A. T. *J. Catal.* **1973**, *31*, 96. [\[ChemPort\]](#)
31. Stone, F. S. *Adv. Catal.* **1961**, *13*, 1.
32. Garner, W. E.; Stone, F. S.; Tiley, P. F. *Proc. R. Soc. London, A* **1952**, *211*, 472.
33. Horn, K.; Hussain, M.; Pritchard, J. *Surf. Sci.* **1977**, *63*, 244. [\[ChemPort\]](#)
34. Wachs, I. E.; Madix, R. J. *J. Catal.* **1978**, *53*, 208. [\[ChemPort\]](#)
35. Christiansen, M.; Thomsen, E. V.; Onsgaard, J. *Surf. Sci.* **1992**, *261*, 179. [\[ChemPort\]](#)
36. Kessler, J.; Thieme, F. *Surf. Sci.* **1997**, *67*, 405.
37. Hollins, P.; Pritchard, J. *Surf. Sci.* **1979**, *89*, 486. [\[ChemPort\]](#)
38. Tracy, J. C. *J. Chem. Phys.* **1970**, *56*, 2798.
39. Bradshaw, A. M.; Pritchard, J. *Proc. R. Soc. London, A* **1970**, *316*, 169. [\[ChemPort\]](#)
40. Baetzold, R. C. *J. Phys. Chem.* **1985**, *89*, 4150. [\[ChemPort\]](#)

41. Fubini, B.; Bolis, V.; Giamello, E. *Thermochim. Acta* **1985**, 85, 23.[\[ChemPort\]](#)
42. Garner, W. E.; Stone, F. S.; Tiley, P. F. *Proc. R. Soc. London, A* **1952**, 211, 472.
43. Efremov, A. A.; Pankratiev, Y. D.; Davydov, Y. D.; Boreskov, G. K. *React. Kinetic., Catal. Lett.* **1982**, 20, 87.[\[ChemPort\]](#)
44. Huang, Y. Y. *J. Catal.* **1973**, 30, 187.[\[ChemPort\]](#)
45. Choi, K. I.; Vannice, M. A. *J. Catal.* **1991**, 131, 22.[\[ChemPort\]](#)
46. Fernandez-Garcia, M.; Gomez Rebello, E.; Guerrero Ruiz, A.; Conesa, J. C.; Soria, J. J. *Catal.* **1997**, 172, 146.[\[ChemPort\]](#)